Supporting Information

Synthesis of ruthenium-graphene quantum dot-graphene hybrid as promising single-atom catalyst for electrochemical nitrogen reduction with ultrahigh yield rate and selectivity

Li Ruiyi,[a] He Keyang,[a] Xu Pengwu,[a] Wang Wendong,[a] Li Nana,[a] Zhu Haiyan,[a] Li Zaijun[a]* and Liu Xiaohao[a]*

Experimental Details

Ammonia determination

The ammonia concentration in electrolyte was detected by indophenol blue method. In a typical procedure, 2 mL of the electrolyte after nitrogen electrochemical reduction reaction was mixed with 2 mL of 1 M NaOH solution containing salicylic acid (5 wt%) and sodium citrate (5 wt%), added 1 mL of 0.05 M NaClO and 0.2 mL of $C_5FeN_6Na_2O$ (1 wt%). After that, the absorbance at 655nm was measured using an UV-vis spectrophotometer. The concentration-absorbance curve was calibrated using standard ammonia chloride solution with a serious of concentrations.

Hydrazine determination

The hydrazine in the electrolyte was measured by the method of Watt and Chrisp. Here, the mixture of para-(dimethylamino) benzaldehyde (0.62 g), HCl (12 mol L^{-1}, 4 mL), and ethanol (40 mL) was used as a color reagent. 2 mL of the electrolyte after electrolysis was mixed with 2 mL of color reagent. The absorbance at 455 nm was determined. The concentration-absorbance curve was calibrated using standard hydrazine hydrate solution with a serious of concentrations.

^{15}N isotope labelling experiment

An isotopic labelling experiment used $^{15}N_2$ with the N15 enrichment of 99% as the feeding gas to clarify the source of NH_3. After $^{15}N_2$ electrochemical reduction for 2 h with 10 cycles, the electrolyte was concentrated into 10 mL, the obtained $^{15}NH_4^+$ was identified by using ^1H NMR spectroscopy (AVANCE III HD 400 MHz).

Figures and Tables

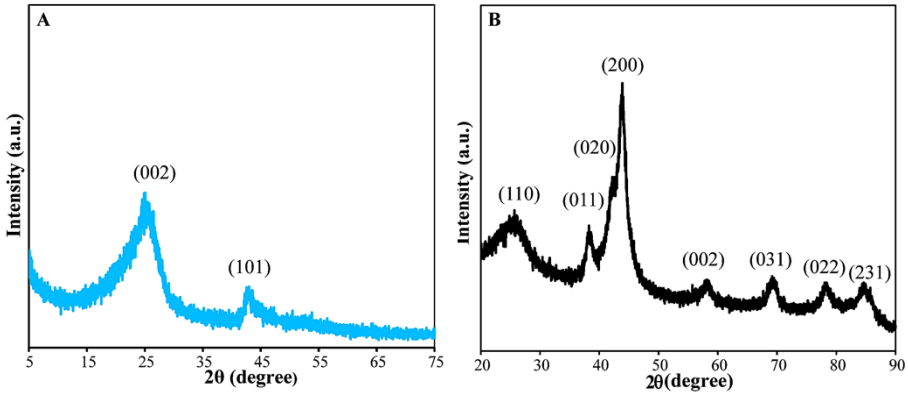

Fig. S1. XRD patterns of Ru-His-GQD-Ru (A) and Ru-graphene nanocomposite (B)

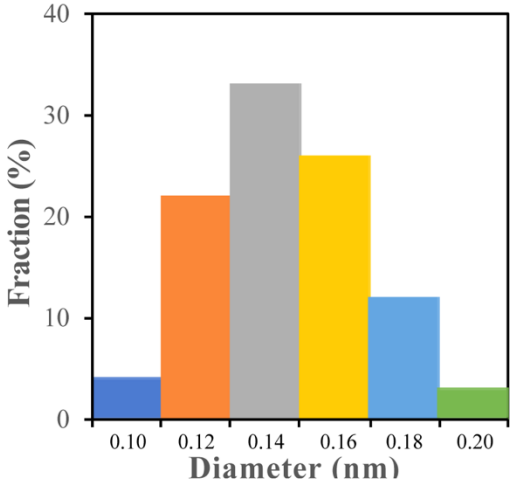

Fig. S2. Size distribution of the Ru particles in Ru-His-GQD-G

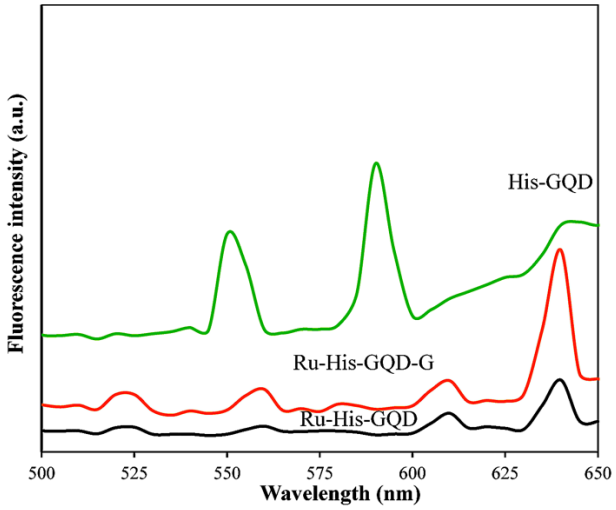

Fig. S3. Solid state fluorescence spectra of His-GQD, Ru-His-GQD and Ru-His-GQD-G

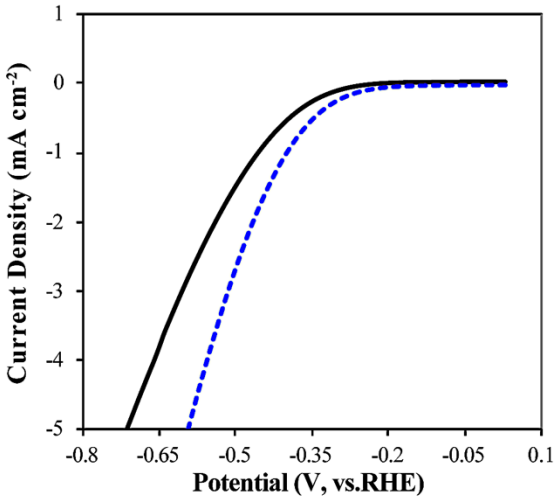

Fig. S4. The linear sweep voltametric curves of Ru-His-GQD-G electrode in Ar- or N_2-saturated 0.05 M aqueous H_2SO_4 at a scan rate of 5 mV s^{-1}

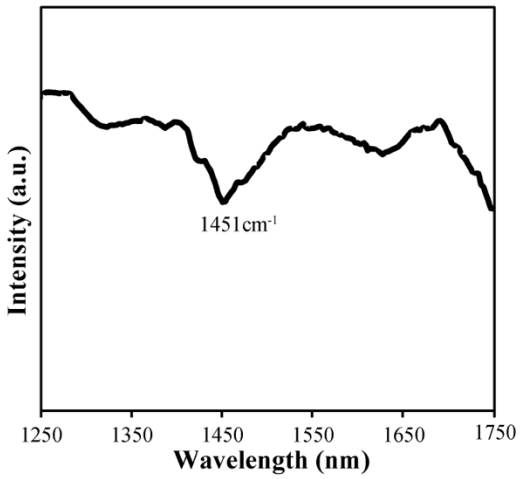

Fig. S5. The FTIR spectrum of the electrolyte for Ru-His-GQD-G. The electrolyte was measured in N_2-saturated 0.05 M H_2SO_4 at -0.05 V vs RHE for 12 h

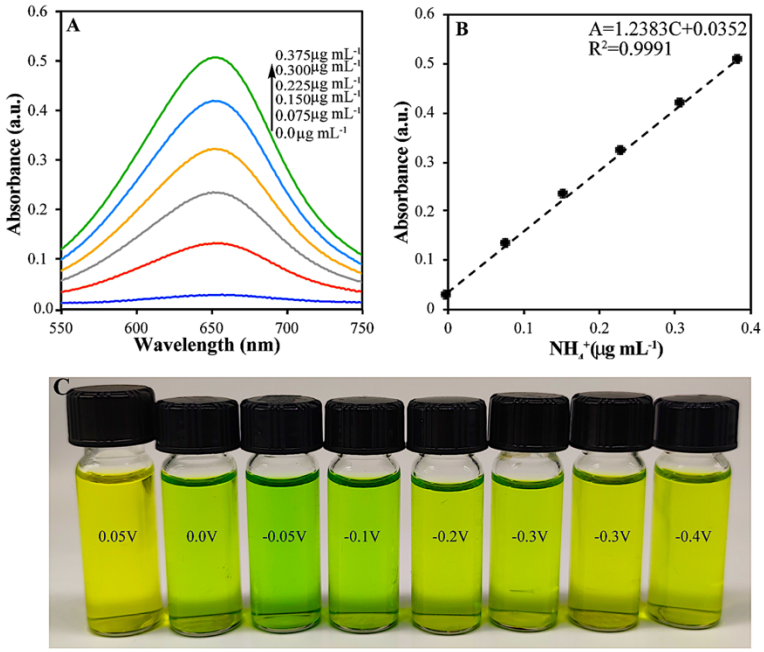

Fig. S6A. UV-vis curves and (b) concentration-absorbance curve of NH_4^+ ions solution with a series of standard concentration. The absorbance at 655 nm was measured by UV-vis spectrophotometer. B: The standard curve showed good linear relation of absorbance with NH_4^+ ion concentration. C: Optical photographs of eight electrolytes prepared by NRR over Ru-His-GQD-G at different potentials for 2 h

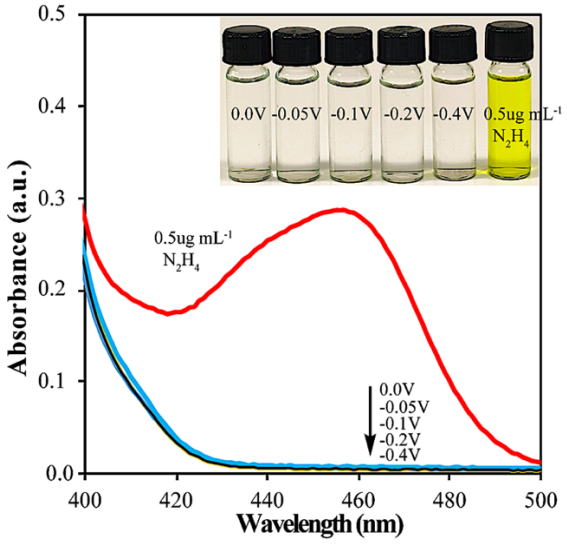

Fig. S7. The UV-vis curves and optical photographs of five electrolytes produced by NRR over Ru-His-GQD-G at different potentials and 0.5μg mL^{-1} $N_2H_4 \cdot H_2O$ standard solution

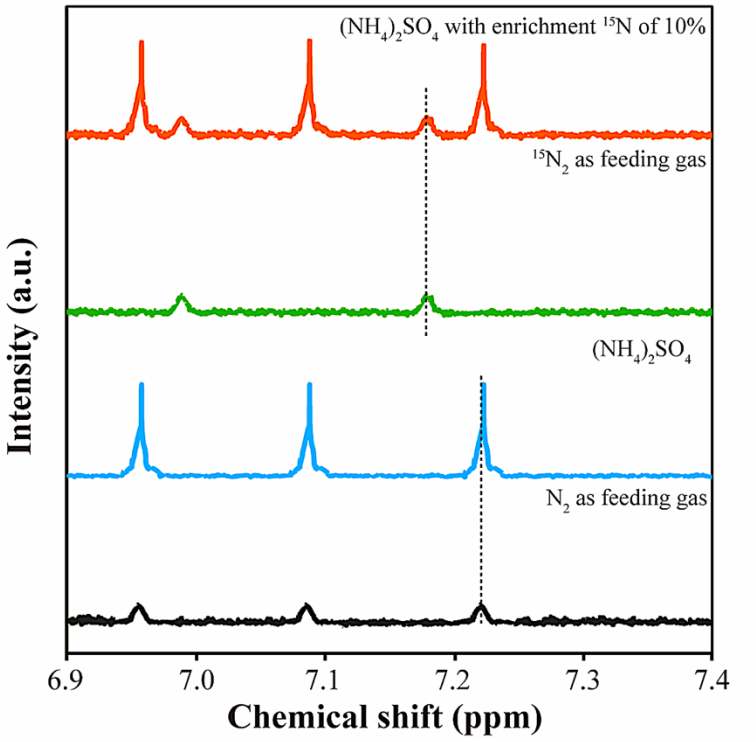

Fig. S8 ^{1}H NMR spectra of both NH_4^+ and $^{15}NH_4^+$ produced from NRR using N_2 and $^{15}N_2$ as the feeding gas

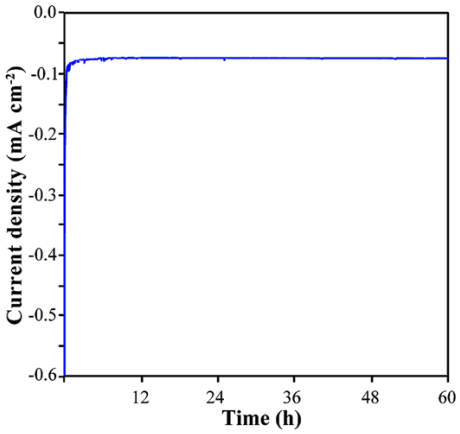

Fig. S9 Current density profile versus time under applied potential of -0.05 V (*vs*. RHE) over Ru-His-GQD-G electrode

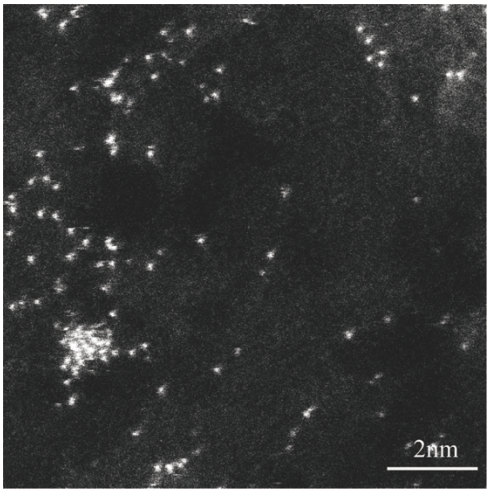

Fig. S10 The HAADF-STEM image of Ru-His-GQD-G after N_2 electrochemical reduction reaction

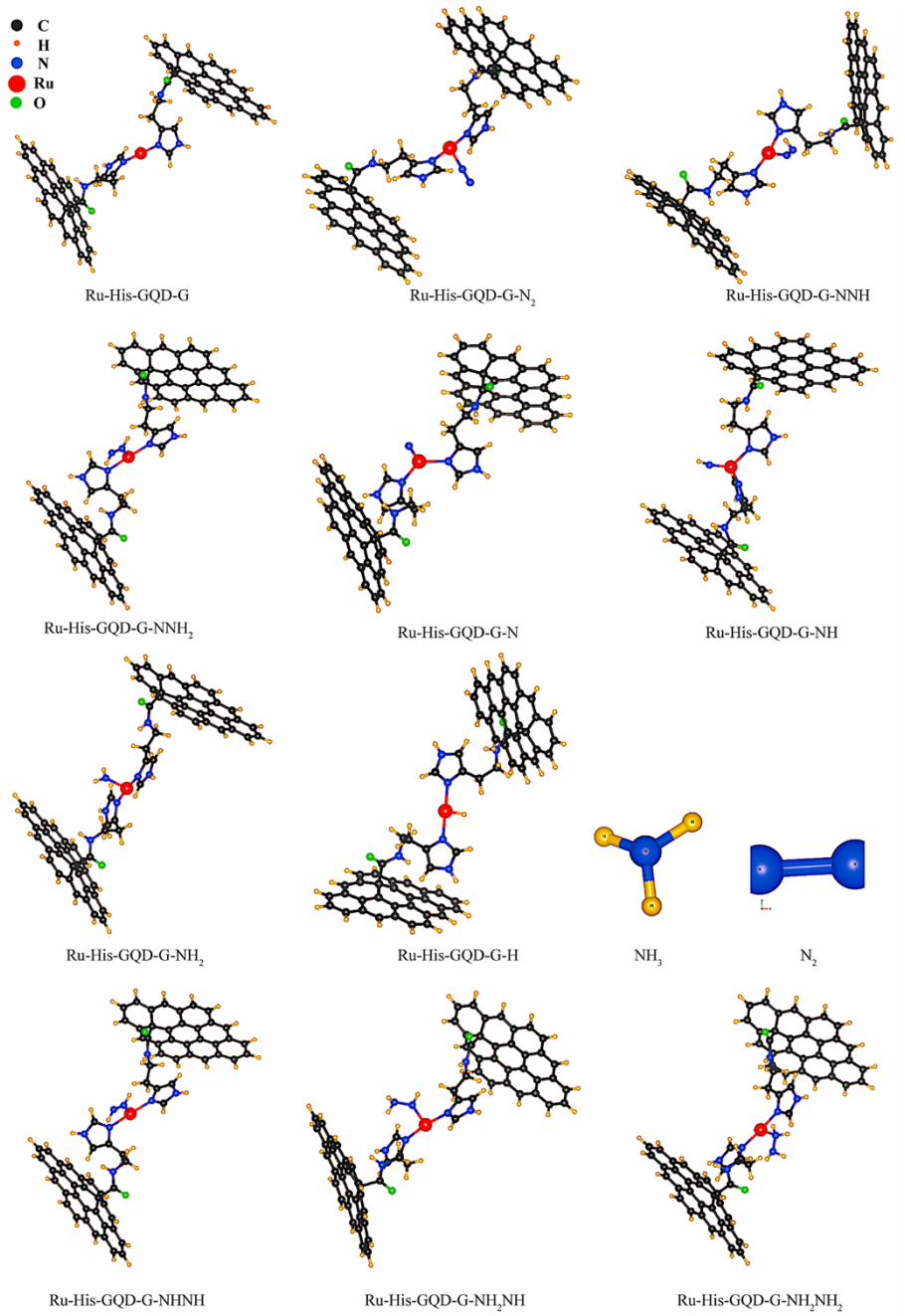

Figu. S11 Optimized geometry of *H and reaction intermediates for NRR on Ru-His-GQD-G electrode

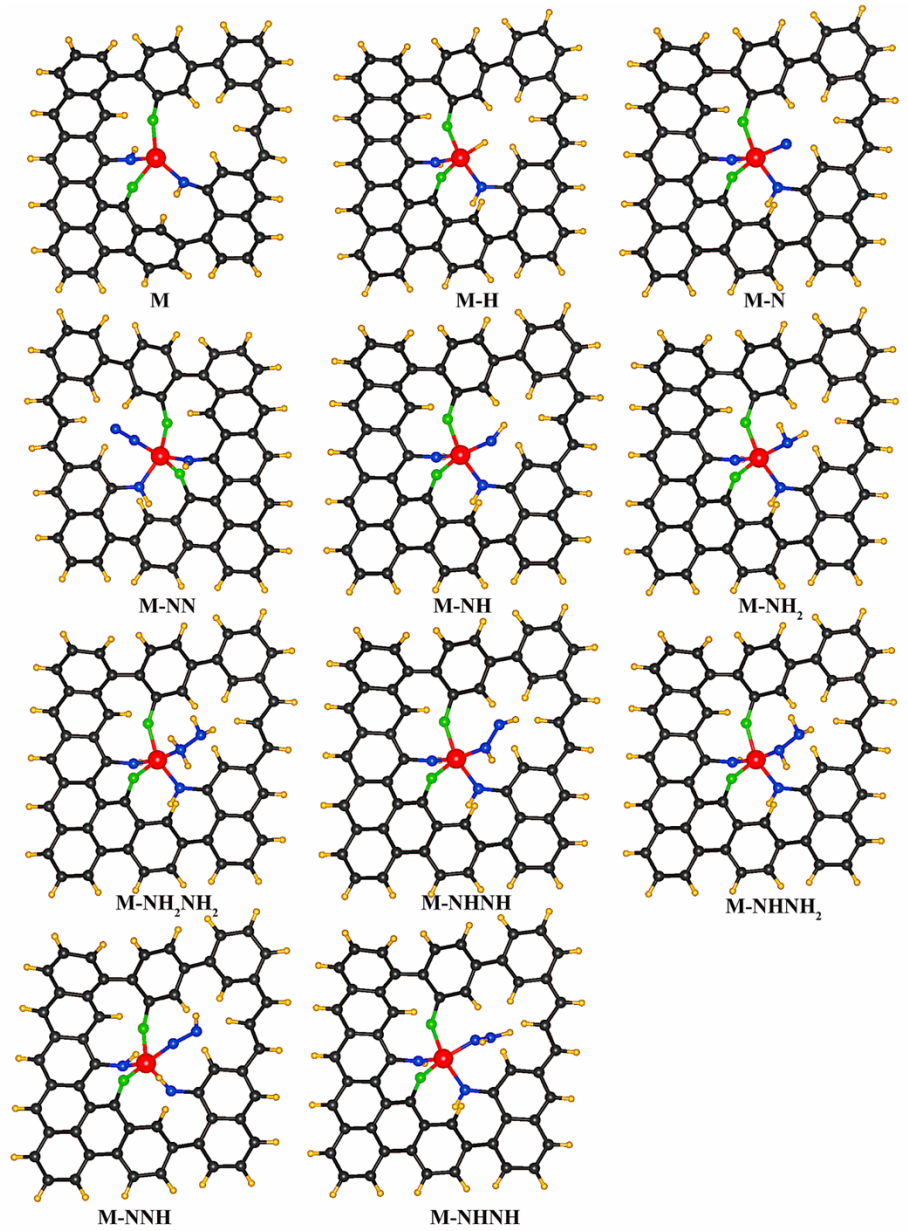

Fig. S12 Optimized geometry of *H and reaction intermediates for NRR on G-Ru electrode

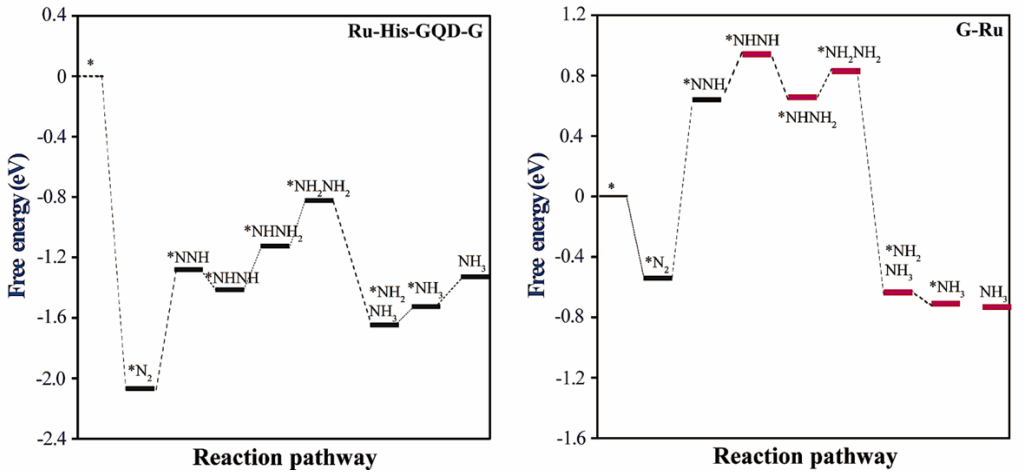

Fig. S13 Calculation models and free energy diagrams for NRR of Ru-His-GQD-G electrode and G-Ru electrode

Table s1 EXAFS data fitting results of Ru foil and Ru-His-GQD-G*

Sample	**Path**	**CN**	**R(Å)**	**σ^2(×10^{-3}Å^2)**	**ΔE_0 (eV)**	**R factor (%)**
Ru foil	Ru-Ru	12	2.67	0.0026 1	-7.767	1.50 %
Ru-His-GQD-G	Ru-N	2.01	2.13	0.01 1	1.93	1.60%

* The EXAFS spectra fits were performed on the first coordination shell over the FT of the k^3-weighted χ(k) function in the Δk= 3-12 Å^{-1} interval. The amplitude reduction factor S_0^2 was fixed to 0.98 relative to Ru foil. The CN represents average coordination number. R represents interatomic distance. **σ^2** represents square variation in path length.ΔE_0 represents edge-energy shift. The R-factor represents the goodness of fit.

Table S2 Catalytic activities of various Ru-based materials for nitrogen electrochemical reduction into ammonia

Catalyst	Electrolyte	Potential (V, *vs.* RHE)	Faradaic Efficiency (%)	N_2 electrochemical reduction activity ($\mu g_{NH_3} \cdot mg^{-1}_{catalyst} \cdot h^{-1}$)	Ref.

Ru single atoms distributed on nitrogen-doped carbon	0.05 M H_2SO_4	-0.2	29.6	120.9	1
Single Ru sites supported on N-doped porous carbon and ZrO_2	0.1 M HCl	-0.21	21	3.665	2
Ru single atoms distributed in a matrix of graphitic carbon nitride	0.5 M KOH	0.05	8.3	23	3
Fusiform-like Ru-Cu alloy nanosheets	0.1 M HCl	-0.1	7.2	53.6	4
Ru(III) polyethyleneimine catalysts supported on carboxyl-modified carbon nanotubes	0.1 M KOH	-0.1	30.93	188.90	5
Single-atomic ruthenium modified Mo_2CTX MXene nanosheets	0.5 M K_2SO_4	-0.3	25.77	40.57	6
Ruthenium nanocrystals anchored on reduced graphene oxide modified with different aliphatic thiols to achieve M-S linkages	0.05 M H_2SO_4	-0.1	11	50	7
Ru-His-GQD-G	).05 M H2SO4	-0.05	42.6	226	Present work

References

1 Z.G. Geng, Y. Liu, X.D. Kong, P. Li, Z.Y. Liu, J.J. Du, M. Shu, R. Si, J. Zeng, *Adv. Mater.*, 2018, **30**, 1803498.

2 H.C. Tao, C. Choi, L.X. Ding, Z. Jiang, Z.S. Han, M.W. Jia, Q. Fan, Y.N. Gao, H.H. Wang, A.W. Robertson, S. Hong, Y. Jung, S.Z. Liu, Z.Y. Sun, Chem, 2019, **5**, 204-219.

3 B. Yu, H. Li, J. White, S. Donne, J.B. Yi, S.B. Xi, Y. Fu, G. Henkelman, H. Yu, Z.L. Chen, T.Y. Ma, *Adv. Funct. Mater.*, 2019, **6**, 1905665.

4 Y. Jin, X. Ding, L.L. Zhang, M.Y. Cong, F.F. Xu, Y. Wei, S.J. Hao, Y. Gao, *Chem. Commun.,* 2020, **56**, 11477-11480.

5 G.R. Xu, M. Batmunkh, S. Donne, H.N. Jin, J.X. Jiang, Y. Chen, T.Y. Ma, *J. Mater. Chem*. *A,* 2019, **7**, 25433-25440.

6 W. Peng, M. Luo, X.D. Xu, K. Jiang, M. Peng, D.C. Chen, T.S. Chan, Y.W. Tan, *Adv Energy Mater.,* 2020*,* **10**, 2001364.

7 M.I. Ahmed, C.W. Liu, Y. Zhao, W.H. Ren, X.J. Chen, S. Chen, C. Zhao, *Angew. Chem*., 2020, **59**, 21465-21469.